Antiprotonic atoms with short-lived nuclei

—— *Obsolete Projects* ——

Michiharu Wada, KEK

pbar-RI at SLOWRI/RIKEN 2003

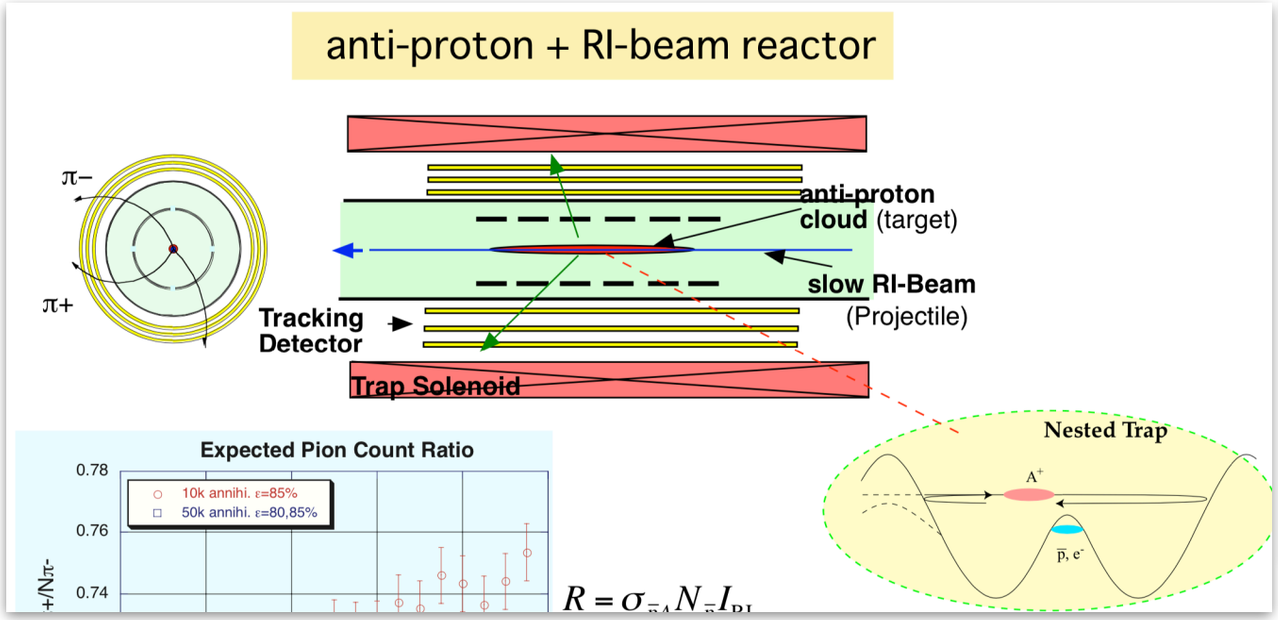

M. Wada, Y. Yamazaki NIMB214(2004)196

- trap pbar @ AD/CERN
- send RIKEN via Siberian Railway
- pbar + halo nuclei @ SLOWRI/RIKEN

too ambitious?

Exo-pbar at FAIR/GSI 2004

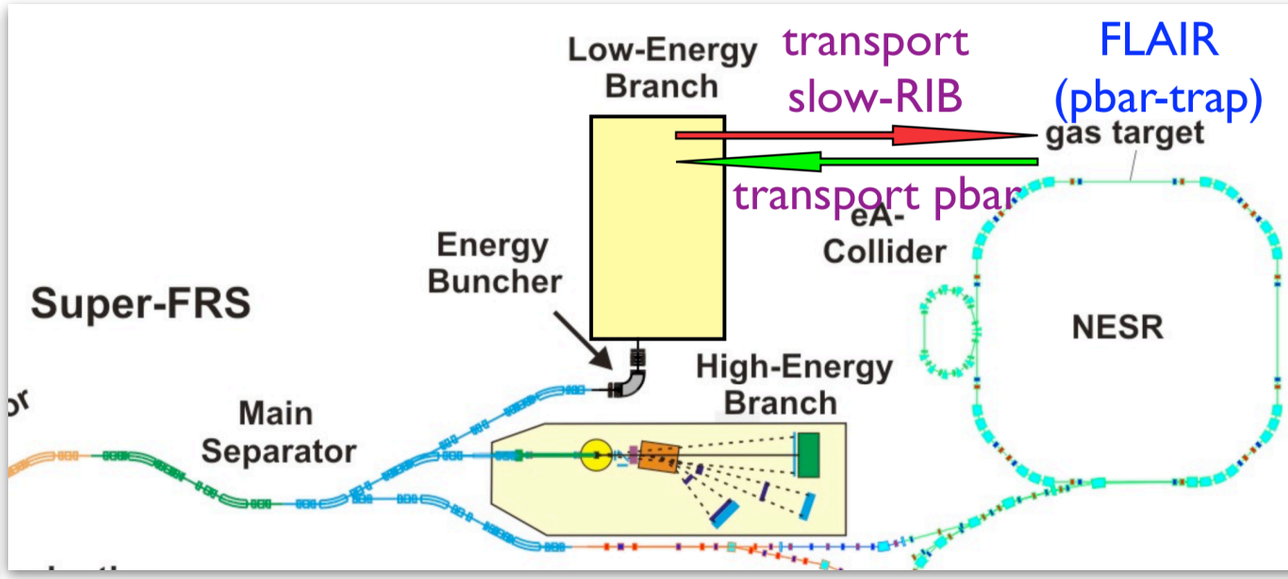

GSI TDR 2005

- trap pbar @FLAIR
- RI-beams from Super-FRS LEB
- pbar + halo nuclei @FAIR

no facilities have been built, no collaboration exists

Motivation

Since 1985, "neutron halo" becomes sensational in nuclear physics

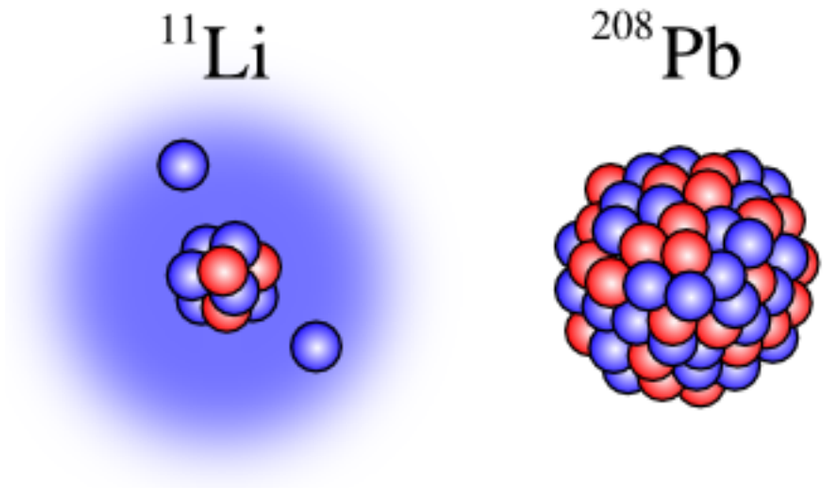

More Spectroscopic or Direct indication?

Interaction Cross Section

↓

Matter Radius

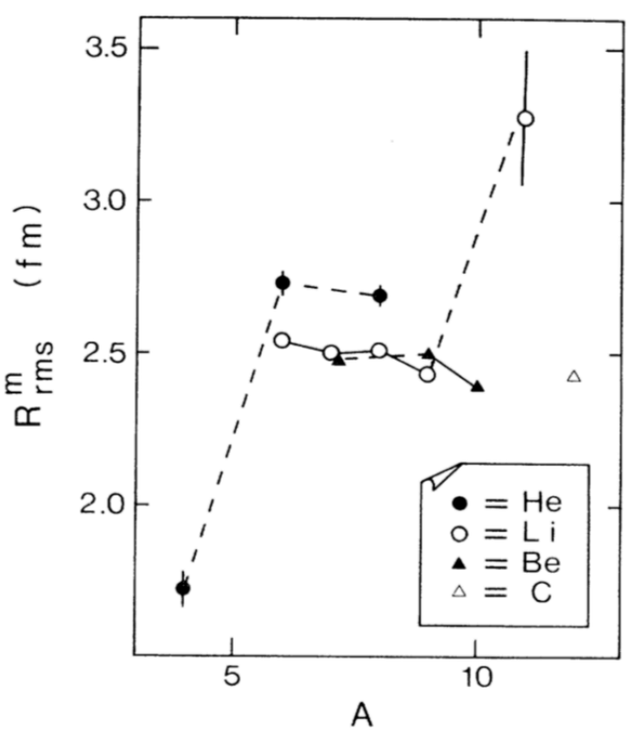

FIG. 3. Matter rms radius R^m_{rms}. Lines connecting isotopes are only guides for the eye. Differences in radii are seen for isobars with $A = 6, 8$, and 9. The ^{11}Li isotope has a much larger radius than other nuclei.

I. Tanihata et al, PRL55(1985)2676

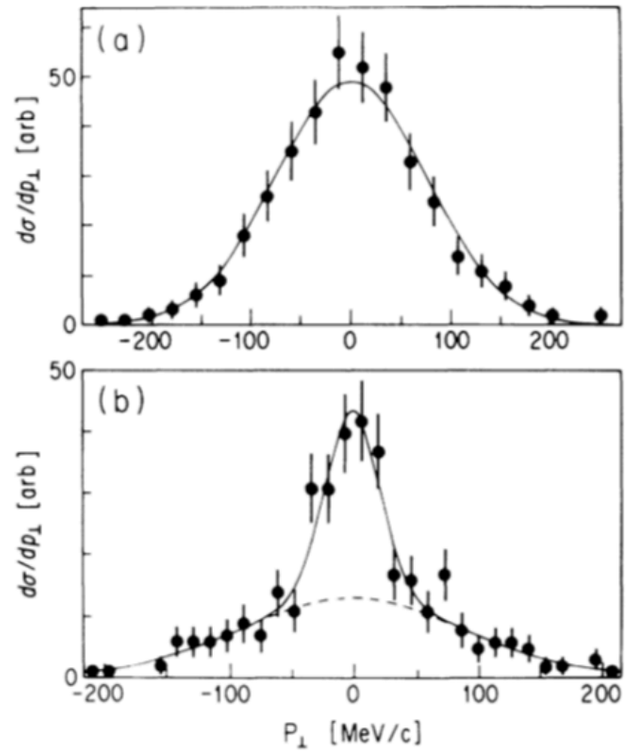

FIG. 1. Transverse-momentum distributions of (a) ^{6}He fragments from reaction ^{8}He+C and (b) ^{9}Li fragments from reaction ^{11}Li+C. The solid lines are fitted Gaussian distributions. The dotted line is a contribution of the wide component in the ^{9}Li distribution.

T. Kobayashi et al, PRL60(1988)2599

Narrow Recoil Momenta

↓

Weakly bound two neutrons

Optical Spectroscopy of neutron halo

Bohr-Weisskopf effect for valence neutron radius

^{11}Be

Z=4
N=7
(T1/2=13s)

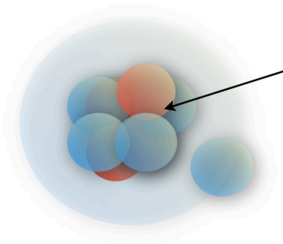

^{10}Be

Z= 4
N= 6

Core + One loosely bound Neutron

Charge Radius

IS (E0)

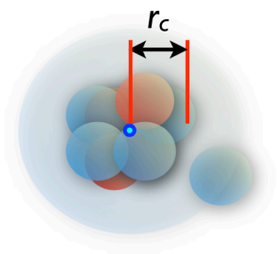

Volume without Charge-less Neutron

Magnetization Radius

IS (M1)

Distribution of Valence Neutron

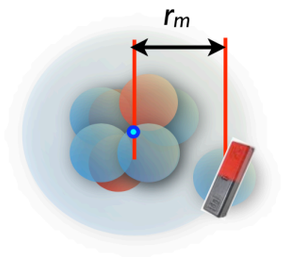

Single Valence Neutron carries most of Magnetization of Nucleus

Cancelled in the Core
(core polarization still exist)

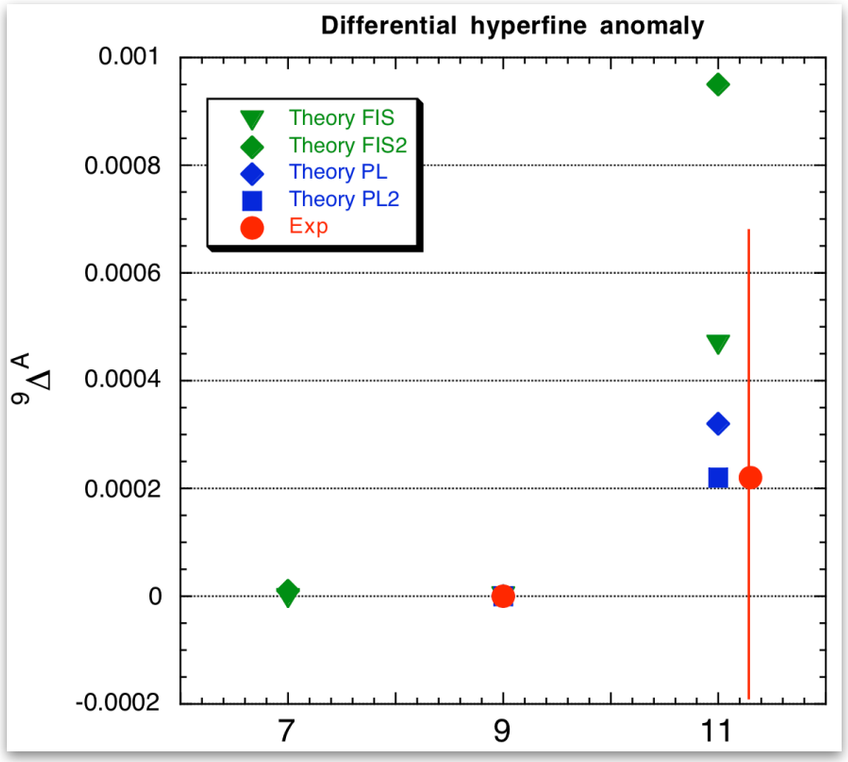

$$^{9}\Delta^{11} = \frac{A_9/\mu_9}{A_{11}/\mu_{11}} - 1 = 2.2(48) \times 10^{-4}$$

	Be7	Be9	Be11
HFS constant A (MHz)	-742.7722(4)	-625.0088370529(11)	-2677.308(2)
Nuclear Mag. Moment (n.m)	[-1.39928(2)]	-1.177432(3)	(-)1.6816(8)*

5x10^-4

* W. Geithner et al, PRL 83(1999)3792

More Universal Method?

K. Okada et al, PRL101(2008)212502 I. Takamine et al, PRL112(2014)162502

Neutron halo from Antiproton absorption

Bubble Chamber experiment in 1973

Evidence for a Neutron Halo in Heavy Nuclei from Antiproton Absorption*

W. M. Bugg, G. T. Condo, and E. L. Hart
The University of Tennessee, Knoxville, Tennessee 37916

and

H. O. Cohn and R. D. McCulloch
Oak Ridge National Laboratory, Oak Ridge, Tennessee 37830

(Received 19 April 1973)

PRL 31(1973)475

From a study of stopping antiprotons in a variety of elements located in a hydrogen bubble chamber, we find evidence for the existence of a neutron fringe in heavy nuclei.

TABLE IV. "Halo factor" analysis.

Element	$N(\pi^-) - N(\pi^+)$	$N(\bar{p}n)$	$N(\bar{p}p)$	$\frac{N(\bar{p}n)}{N(\bar{p}p)}$	$\frac{N(\bar{p}n)}{N(\bar{p}p)}\Big\|_c$	$\frac{N}{Z}$	Halo factor
C	2302	2586	4089	0.632	1.00	1.00	1.00
Ti	881	1067	1111	0.960	1.52	1.18	1.29 ± 0.21
Ta	1006	1276	931	1.371	2.17	1.48	1.46 ± 0.24
Pb	947	1216	534	2.270	3.59	1.54	2.34 ± 0.50

Charged Pion Ratio

"Calibrate" Rnp by C-12

$$R_{\mathrm{np}} \equiv \sigma_{\bar{p}n}/\sigma_{\bar{p}p} \approx 0.63$$

$$f_{n\mathrm{halo}} = \frac{N(\bar{p}n)}{N(\bar{p}p)} \cdot \frac{Z}{N} \cdot \frac{\sigma_{\bar{p}p}}{\sigma_{\bar{p}n}}$$

Antiprotonic atoms of stable nuclei by Warsaw Group

Radiochemical identification: Halo factor

Jastrzebski et al, NPA 558(1993)405c

Table 1
Summary of ^{232}Th evaluation

	Nuclei per 1000 $\bar{p}$			
	Experiment		Theory, INC [24]	
^{231}Th($\bar{p}$n)	100 ± 27	113	19.5	33
^{231}Ac($\bar{p}$p)	12.9 ± 1.6		13.3	
$\frac{N(\bar{p}n)}{N(\bar{p}p)}$	7.8 ± 2.2		1.5	

$$f(\text{peripheral}) \stackrel{\text{def.}}{=} \frac{N(\bar{p}n)}{N(\bar{p}p)} \frac{Ima_p}{Ima_n} \frac{Z_t}{N_t} = (7.8 \pm 2.2) \frac{1}{0.63} \frac{90}{142} = 7.8 \pm 2.2$$

Cascade X-rays limit: Nuclear size

Hartmann et al, PRC 65(2001)014306

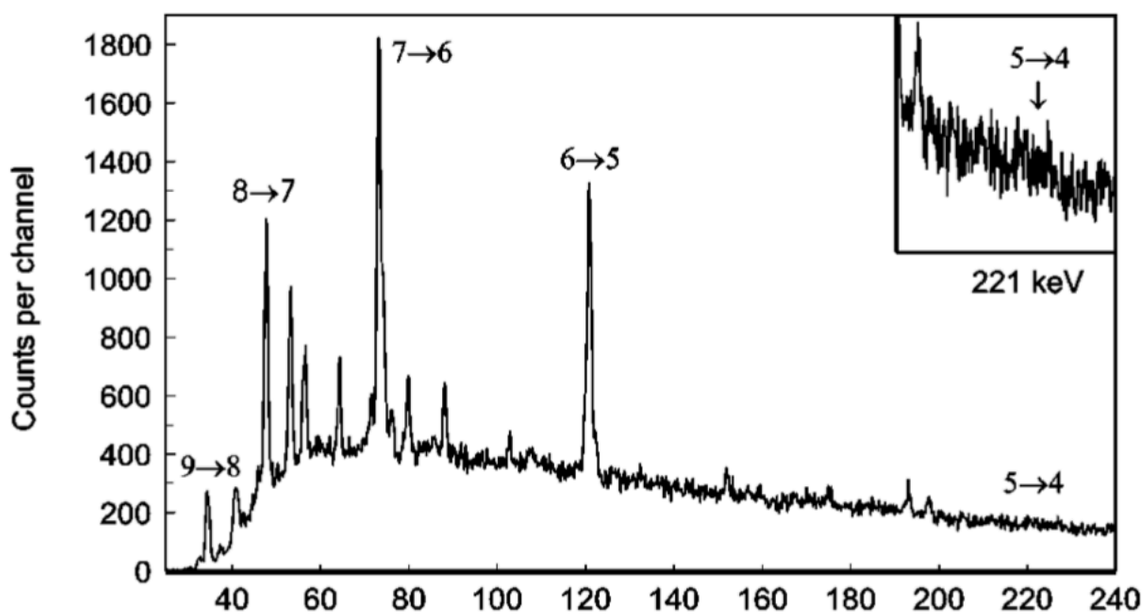

$r_n - r_p$ vs. $(N-Z)A$ Trzcinska et al, PRL 87(2001)082501

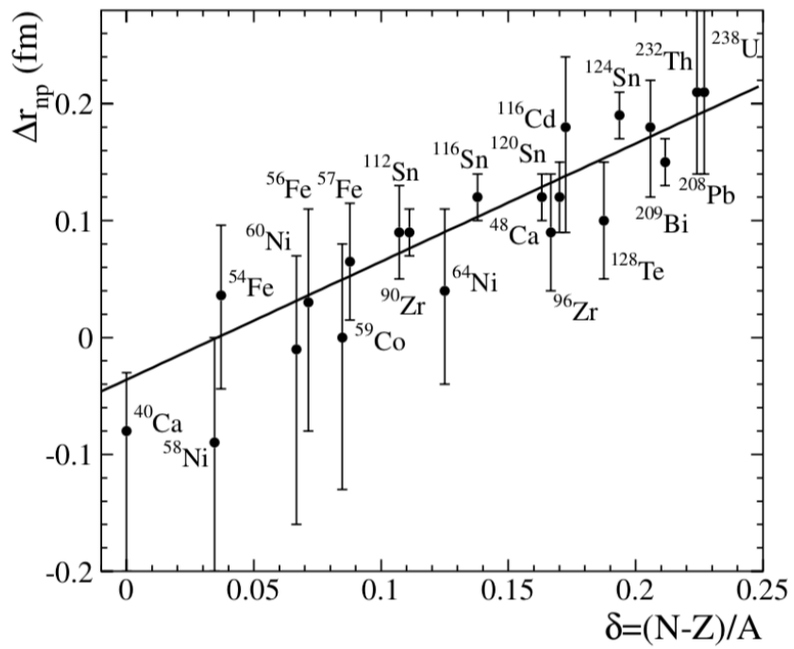

FIG. 4. Difference Δr_{np} between the rms radii of the neutron and proton distributions as deduced from the antiprotonic atom x-ray data, as a function of $\delta = (N - Z)/A$. The proton distributions were obtained from electron scattering data [41] (Sn nuclei) or from muonic atom data [38,42,43] (other nuclei). The

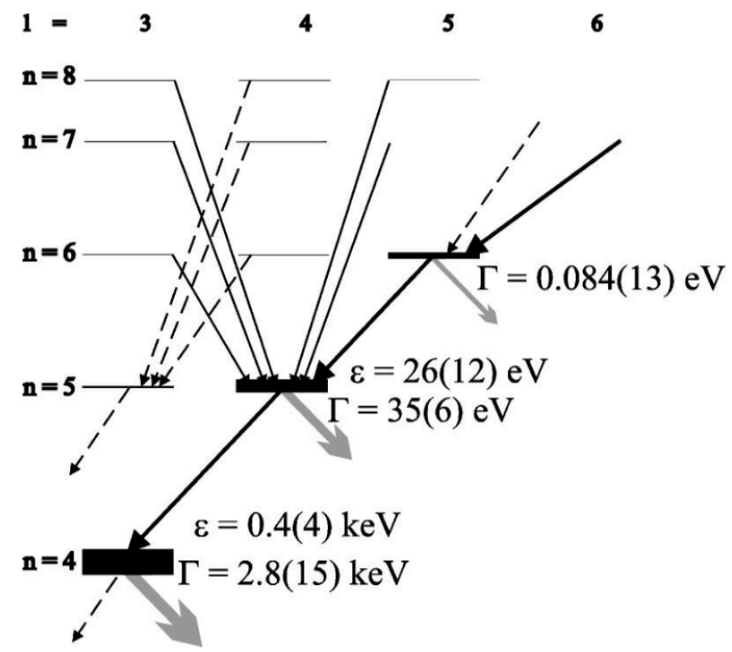

FIG. 3. Mean widths and shifts of all levels with measurable strong interaction effects. The weight of the different calcium isotopes is given in the caption of Fig. 1.

Antiprotonic radioactive atoms (Exo+pbar)

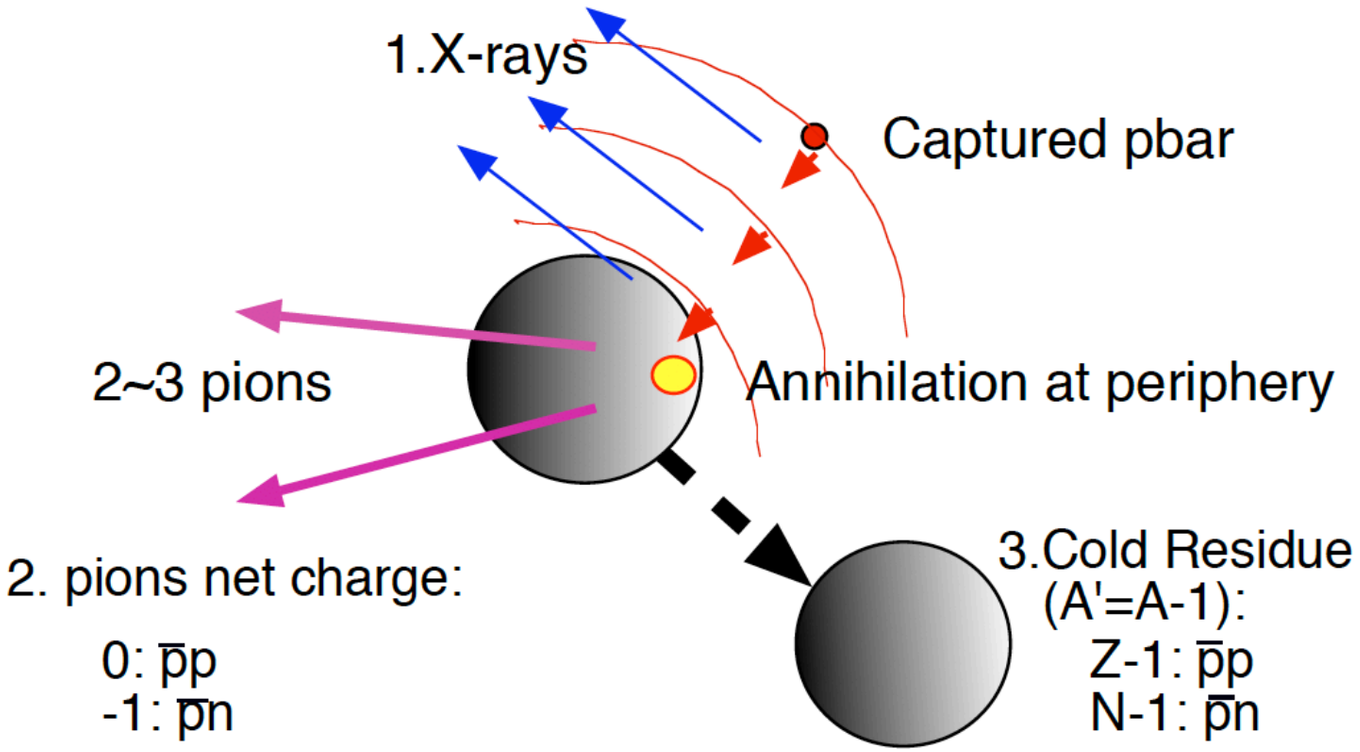

A new probe for nuclear structure study of unstable nuclei

*** annihilation at** $\rho \approx \rho_0 1/1000$

*** pbar distinguishes p and n**

physical quantity	***observable***	***method***	***for RIB****	***previous works for stable nuclei***
nuclear size	X-ray (min. n,l)		?	Trzcinska et al, PRL87(2001) 82501
p,n abundance at nuclear surface	pion net charge	calorimetric		Bugg et al, bubble chamber exp. for C,Ti,Ta,Pb. PRL31(1973)475
		statistical	O	
	cold residue	gamma-ray		Jastrebski et al, PRC47(1993)216
		recoil momentum PI	O	
surface nucleon's momentum	cold residue	recoil momentum	O	

* *radioactive nuclei require efficient detection methods*

Production of pbar-RI atom

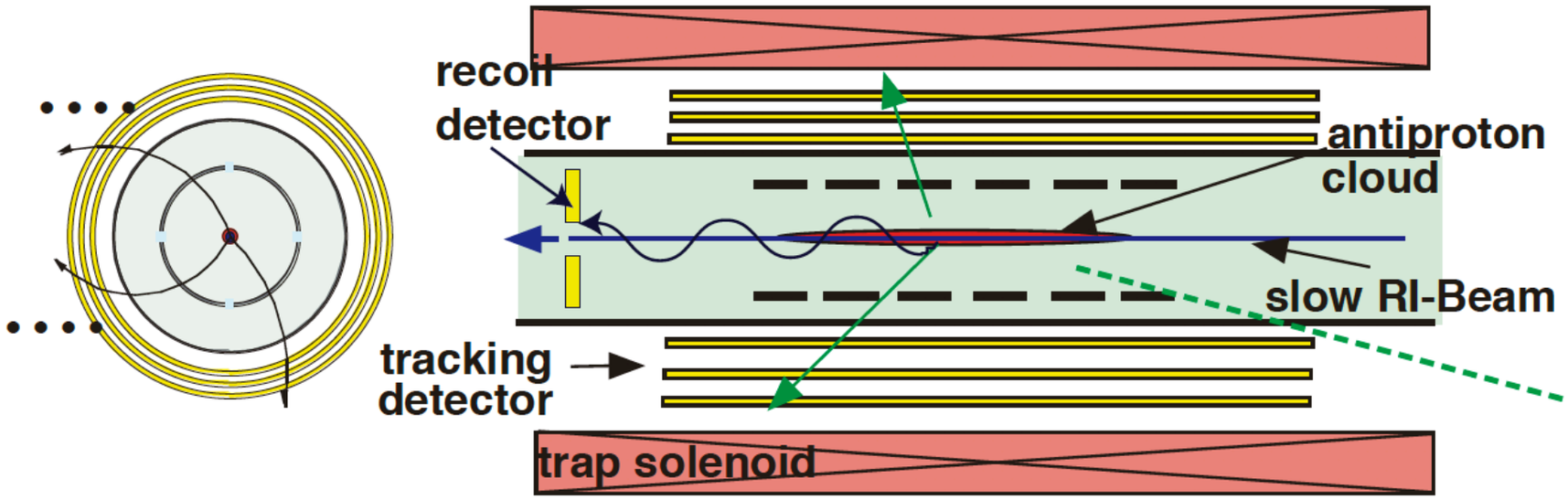

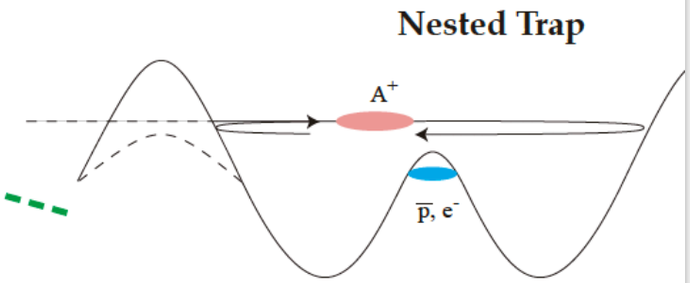

M.Wada, Y.Yamazaki, NIM B214 (2004) 196-200

Capture Cross Section

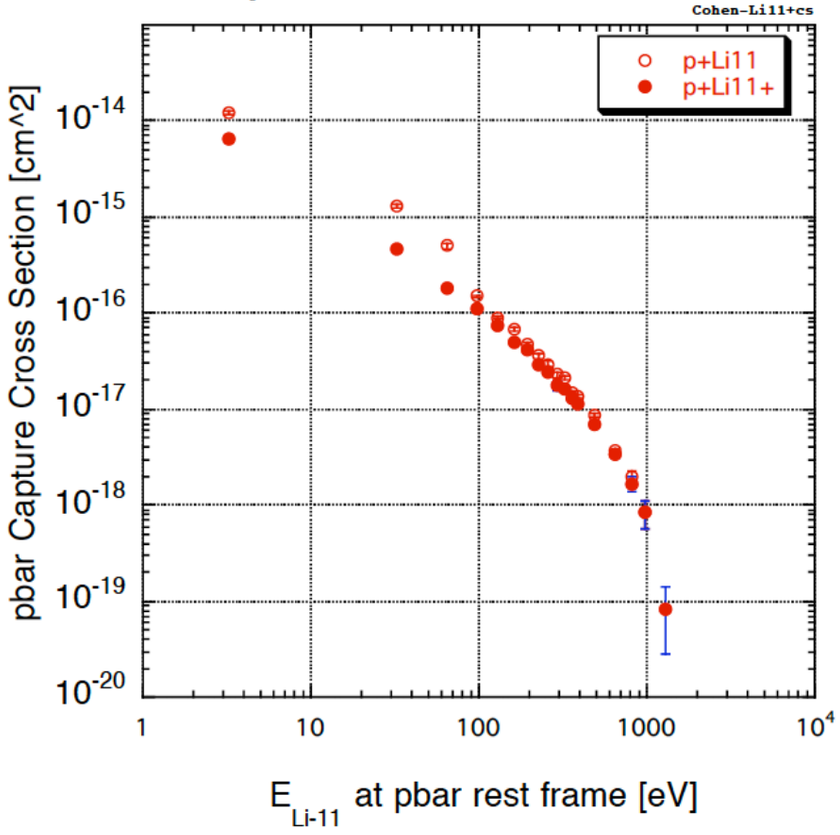

Cohen PRA69(2004)022501

Yield estimation:

5M pbar (target) + 1 k atom/s Li-11, 10ms cycle

$$R = \sigma_{\bar{p}A} N_{\bar{p}} I_{\mathrm{RI}}$$

$$= 4\times10^{-16}[\mathrm{cm}^2]\cdot 5\times10^{8}[\mathrm{cm}^{-2}]\cdot 10[\mathrm{atoms}]\cdot 5\times10^{3}[/10\mathrm{ms}]$$

$$= 1\times10^{-2}[\bar{\mathrm{p}}\mathrm{RI}/10\mathrm{ms}]$$

$$\bar{\mathrm{p}}^{11}\mathrm{Li}^{2+} : 1 \text{ atom/s}$$

Measurement Methods

1. Pion's net charge $\bar{p}p$:0 $\bar{p}n$:−1

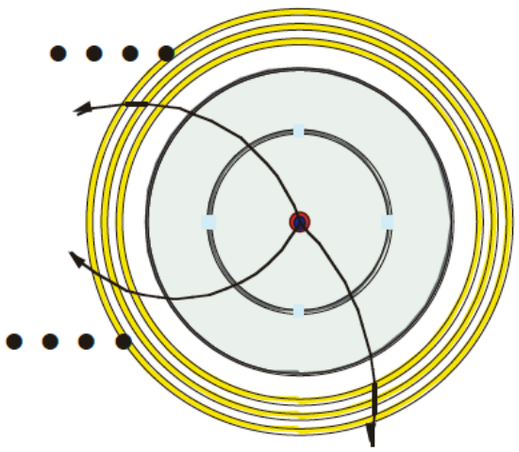

a) Calorimetric detection of charged pions
- O 1 event distinguishes pbar-p or pbar-n annhilations
- X Detection efficiency must be unity.

b) Comparison of statistical sum of detected pions

$$\frac{N(\pi^-)-N(\pi^+)}{N(\pi^-)+N(\pi^+)} \text{ or } \frac{N(\pi^-)}{N(\pi^+)} \Rightarrow \frac{N(\bar{p}n)}{N(\bar{p}p)} \Rightarrow \left.\frac{\rho(n)}{\rho(p)}\right|_{@\ \text{annilation}}$$

* Universal method
* High statistics is needed
* Background pion should be avoided
  (e.g. coincidence with recoil nucleus)

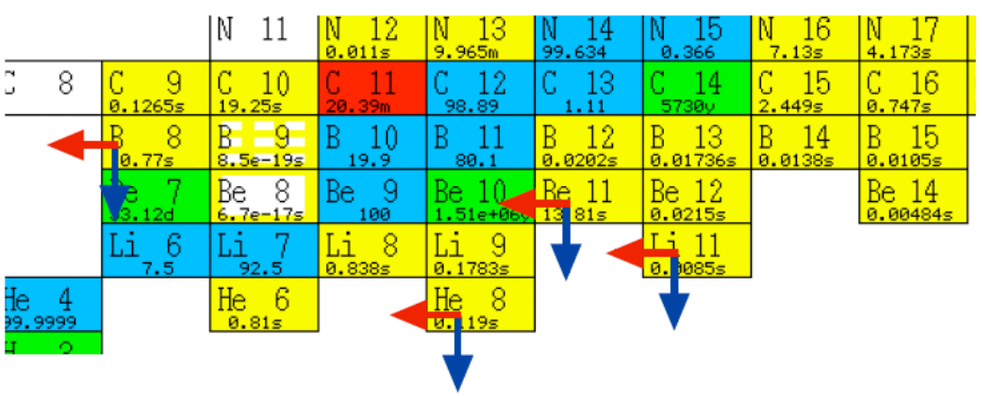

cold residues are often particle unbound

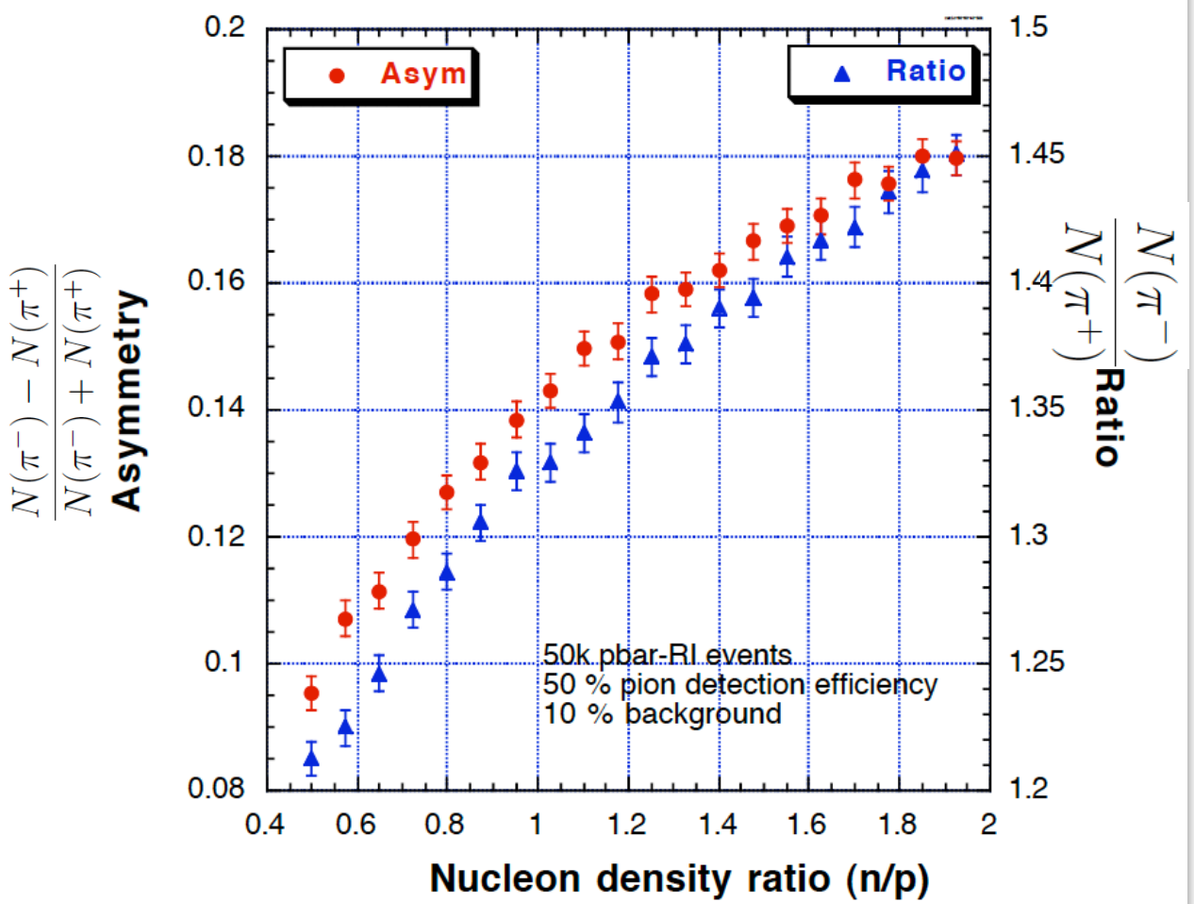

~5% accuracy with 50 k pbar-RI atoms

More detailed statistical treatment including Multiplicity

TABLE 3. Simulated histogram of the multiplicity of charged pions (row) and the total charge per event (column) in a typical experimental condition: $R_{n/p} = 1.0$, $\varepsilon_+ = \varepsilon_- = 0.6$, $\omega_+ = \omega_- = 0.1$, $\lambda_+ = \lambda_- = 0.1$. The number of total annihilation event is 10^5.

$M \backslash \Sigma_c$	-5	-4	-3	-2	-1	0	+1	+2	+3	+4	
0	0	0	0	0	0	0	0	0	0	0	(11386)*
1	0	0	0	0	17223	0	11233	0	0	0	28456
2	0	0	0	7530	0	21437	0	2844	0	0	31811
3	0	0	1029	0	11901	0	6591	0	179	0	19700
4	0	44	0	1904	0	4394	0	519	0	5	6866
5	1	0	99	0	979	0	451	0	13	0	1543
6	0	2	0	75	0	133	0	14	0	0	224
7	0	0	1	0	7	0	3	0	0	0	11
8	0	0	0	1	0	1	0	0	0	0	2
9	0	0	0	0	1	0	0	0	0	0	1
	1	46	1129	9510	30111	25965	18278	3377	192	5	88612

* unobservable events

ω_-, ω_+ : absorption of π^-, π^+ with residue

λ_-, λ_+ : charge exchange π^-, π^+ with residue

nuisance effects can be evaluatable by including multiplicity

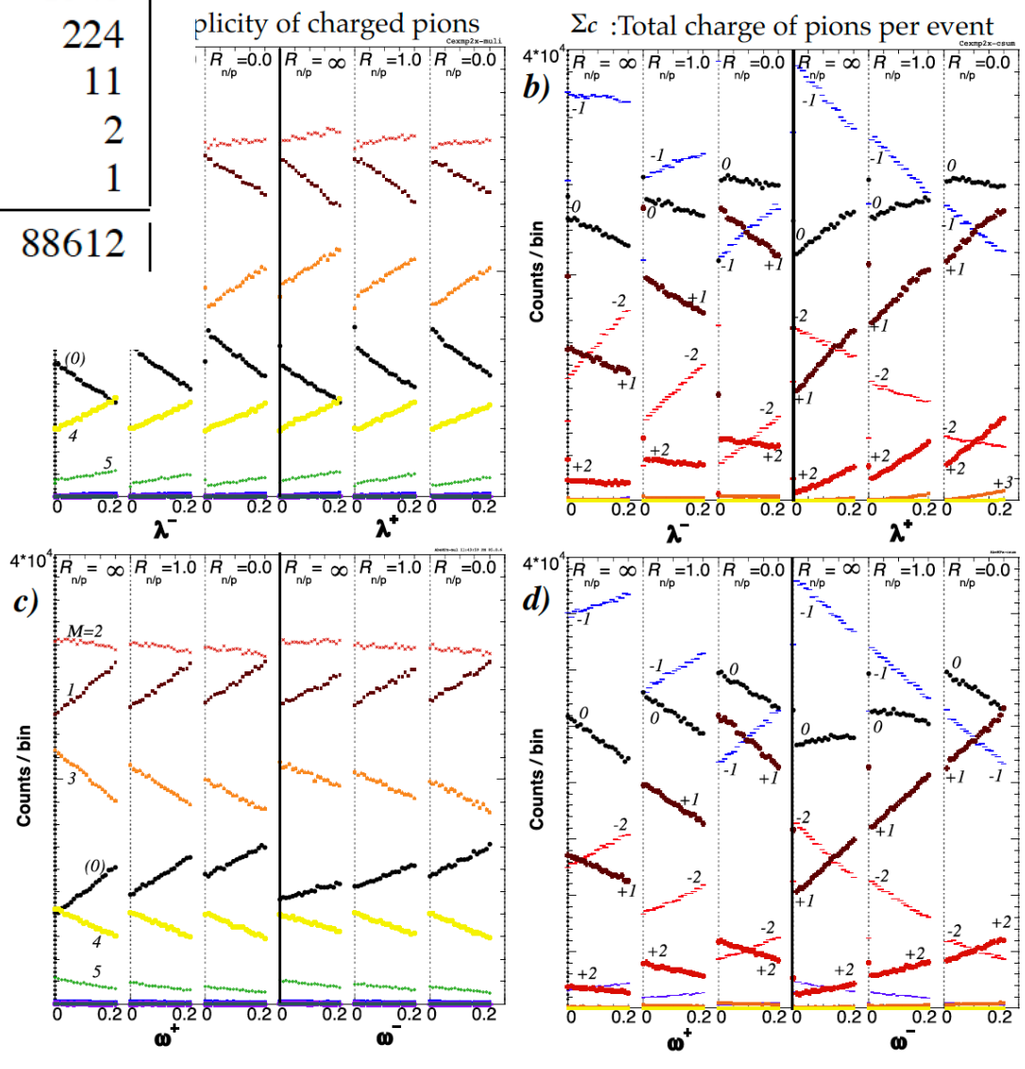

FIGURE 5. Simulation of the dependence of the detected charged pion's multiplicity (left (a, c)) the total charge per event (right (b, d)) on the charge exchange probability $\lambda_\pm$ (top (a, b)) and on absorption probability $\omega_\pm$ (bottom (c, d)). For a) and b), λ_- and λ_+ are scanned from 0.0 to 0.2 w other parameters are fixed: $\varepsilon_\pm = 0.6$, $\omega_\pm = 0.1$ and $\lambda_+ = 0.1$ for left three scans ($\lambda_- = 0.1$ for right t

Wada, Yamazaki, AIP Conference Proceedings **793**, 233 (2005)

Measurement Methods

2. Recoiled Cold Residue

$\bar{p}p: {}^{A-1}_{N}(Z-1)$ $\bar{p}n: {}^{A-1}_{N-1}(Z)$

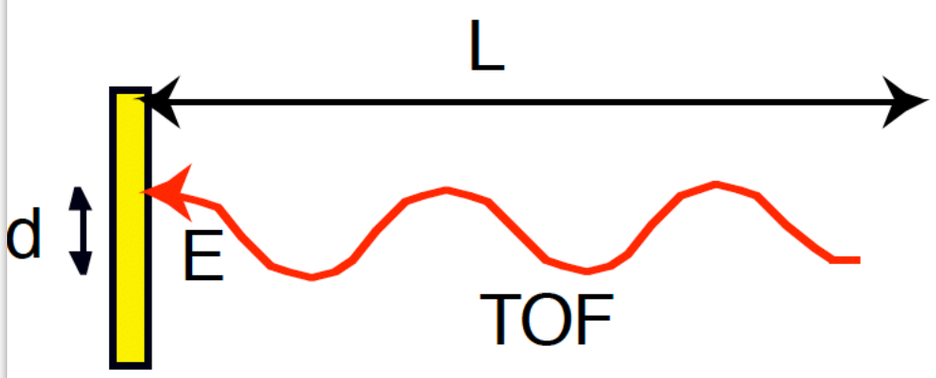

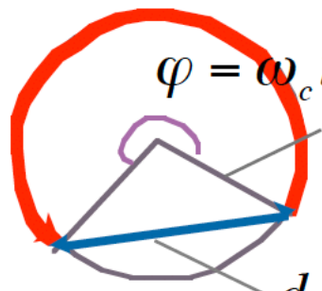

$$\varphi = \omega_c t \qquad \rho = \frac{m|v_r|}{qB}$$

$$d = 2\rho\left|\sin\frac{\varphi}{2}\right|$$

$$d = 2\frac{m}{qB}\sqrt{\frac{2E}{m} - \left(\frac{L}{tof}\right)^2}\left|\sin\left(\frac{qB}{2m}tof\right)\right|$$

Particle Identification &
Momentum measurement

direct deduction of pbar-p, pbar-n
event ratio

$$\frac{N\left({}^{A-1}_{N-1}Z\right)}{N\left({}^{A-1}_{N}(Z-1)\right)} \approx \frac{N(\bar{p}n)}{N(\bar{p}p)}$$

* Higher sensitivity
* Ambiguity due to
  nuclear excitation, re-scattering etc
* Recoil momentum ≈ ***P***vanished nucleon
  + other effects

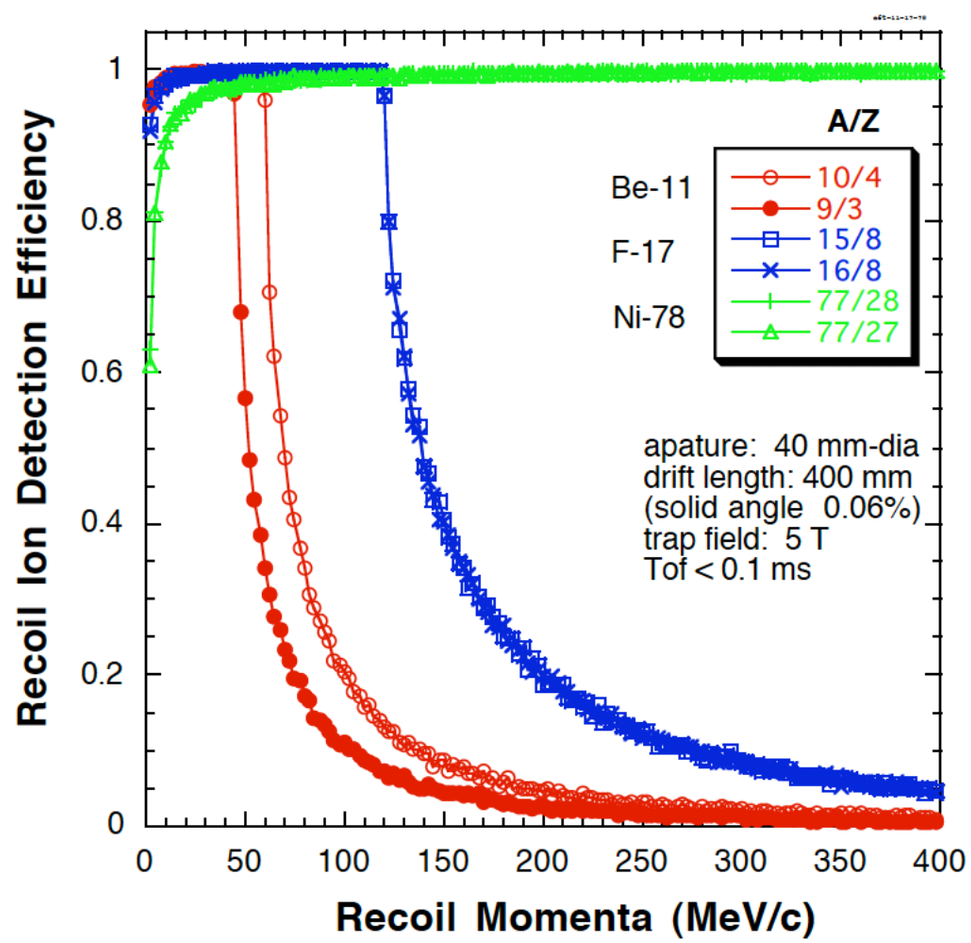

Possible Experimental Locations

1. @CERN AD
   ISOLDE (RI-Beam) ➡ L.E. Beam Transport ➡ AD (pbar)

PUMA2 ?

2. @CERN ISOLDE
   CERN AD(pbar) Portable Trap ➡ ISOLDE (RI-Beam)

PUMA

Loading/Unloading ~2 hours

+ 10 hours ?

3. @RIKEN
   CERN AD(pbar) Portable Trap ➡ RIKEN-RIBF(RI-Beam)

4. @GSI FAIR
   SuperFRS-LEB (RI-Beam) BTL ➡ FLAIR (pbar)

Experimental Locations @FAIR, GSI

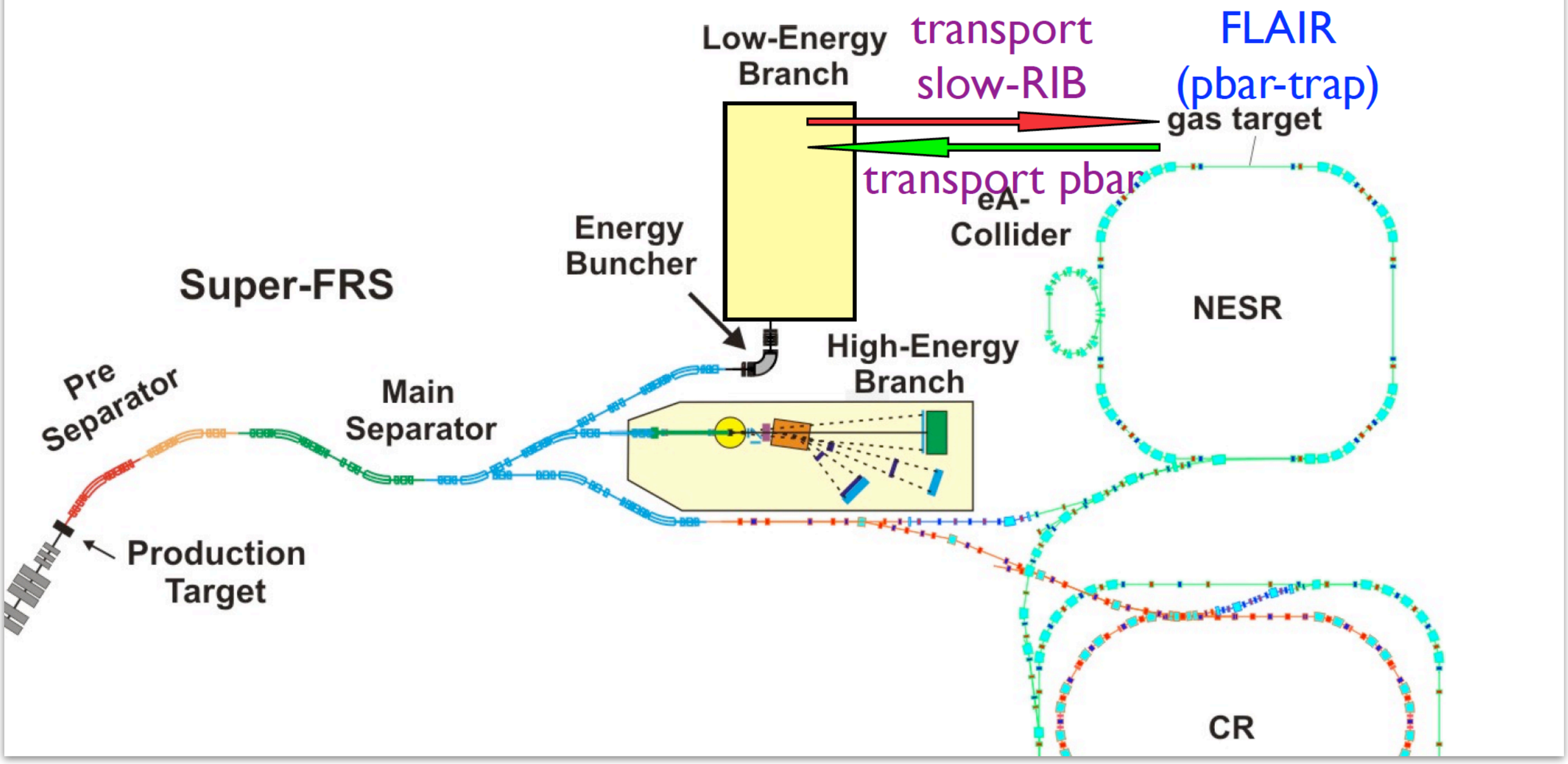

Beam Transport between Super FRS LEB and FLAIR

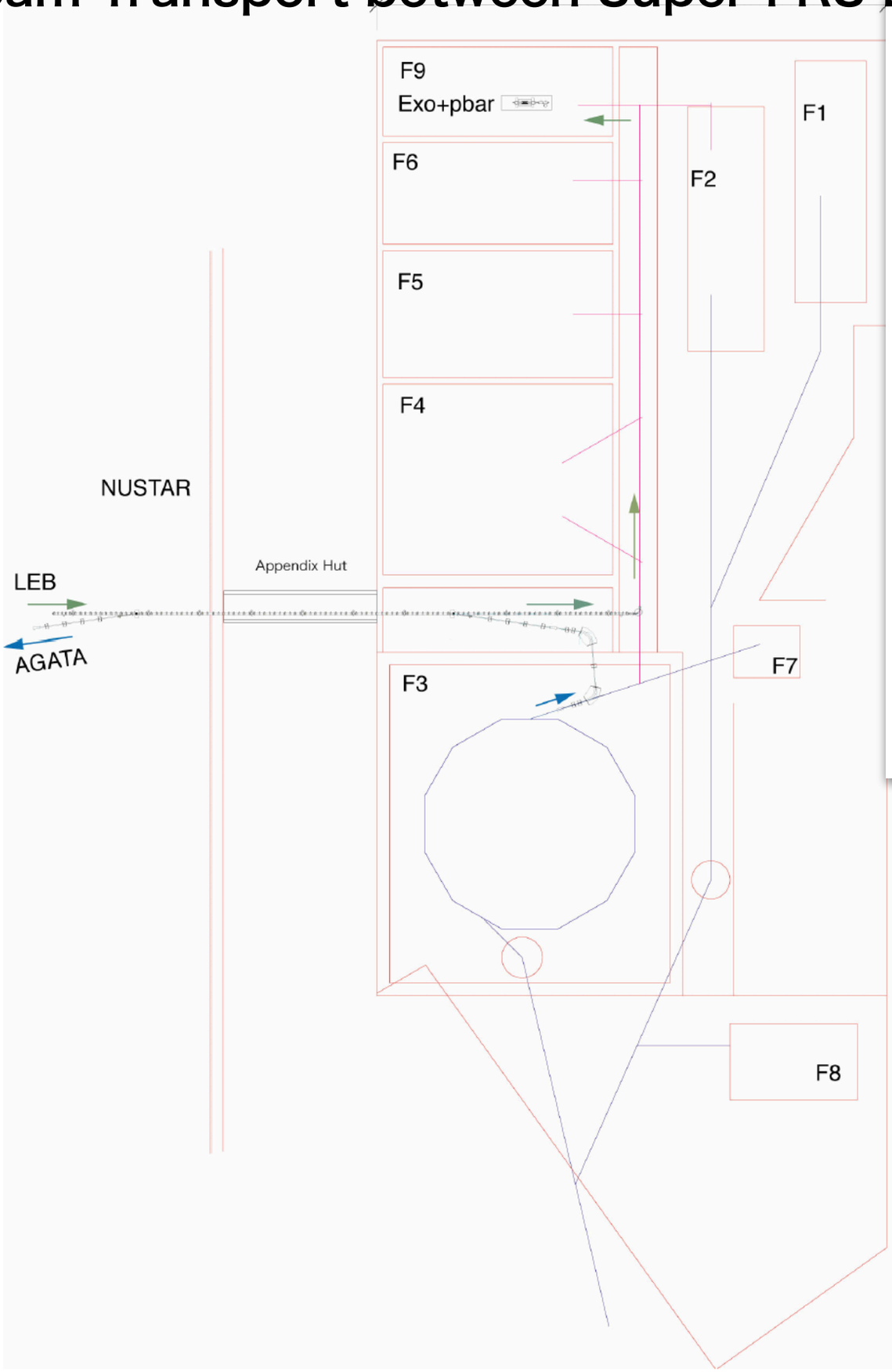

Fig. 88: Long low-energy beam transport line (LBTL) between NUSTAR and FLAIR

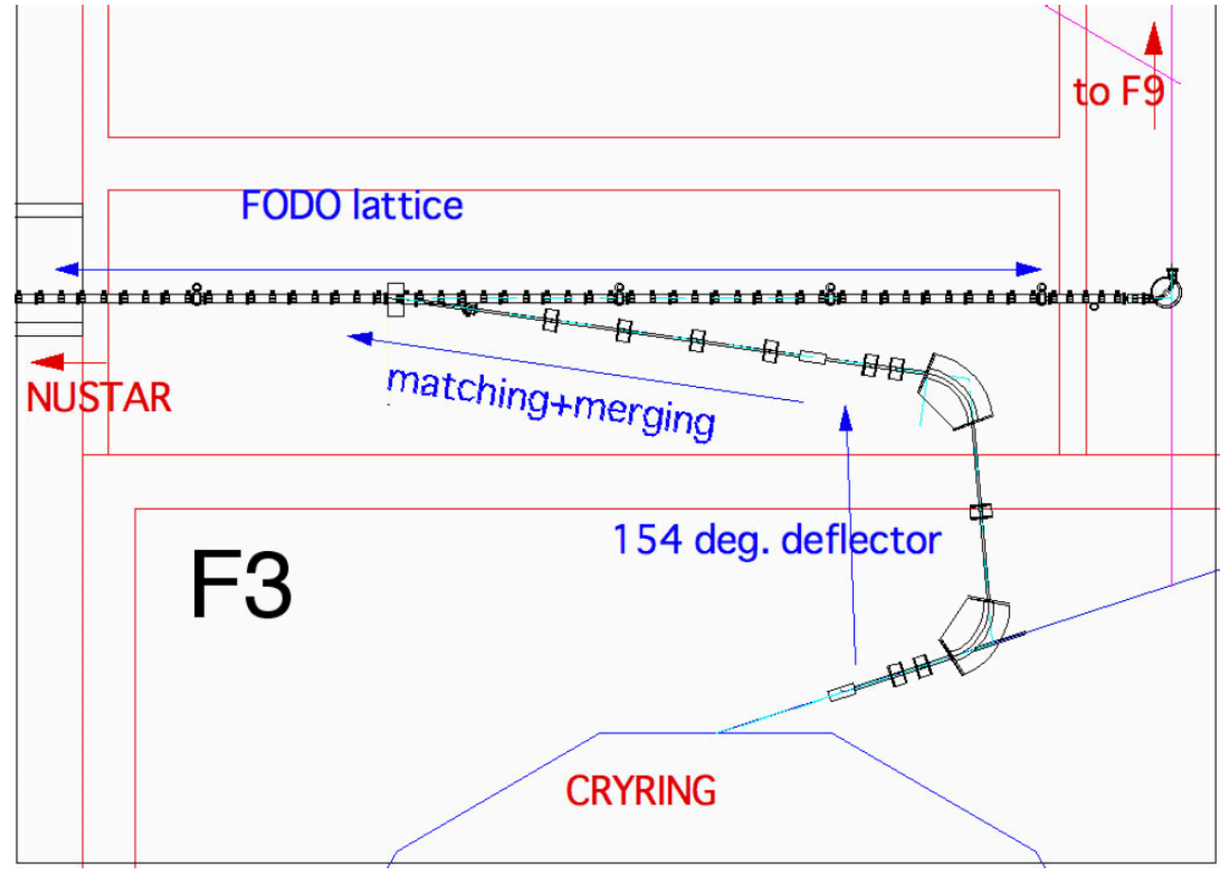

Fig. 89: Core part of LBTL in FLAIR building

GSI TDR 2005

Optics of bi-directional BTL for Heavy Ions and Antiprotons

Table 28: Characteristics of the beams to be transported

	Energy	Emittance	Magnetic Rigidity	Electrostatic Rigidity
Low energy RIB M^{1+}	30 keV	~50 π mm mrad	~0.2 Tm	60 kV
Medium energy RIB $^{200}Au^{79+}$	~6A MeV	< 5 π mm mrad	~0.9 Tm	~30 MV

Heavy Ion

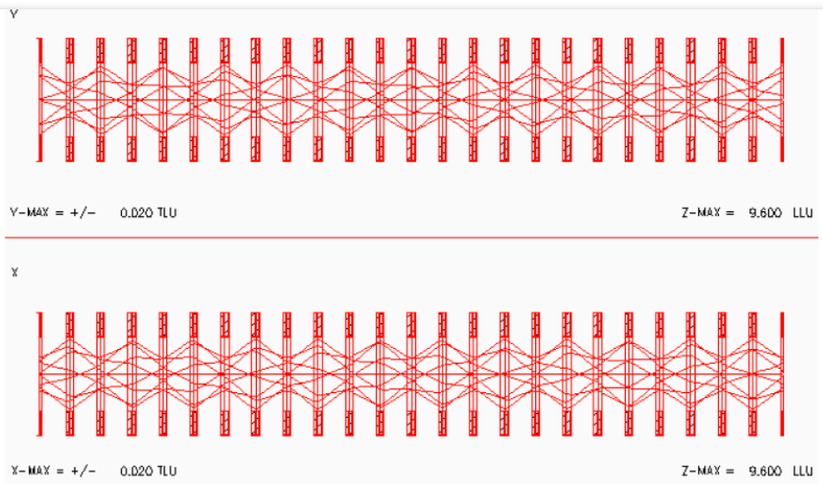

Fig. 90: Part of the beam optics design for low-energy RIB (30 keV, A^+, 60 π mm mrad). Electrostatic quadrupoles with an aperture diameter of 24 mm and a length of 100 mm are placed with a period of 400 mm.

Antiproton

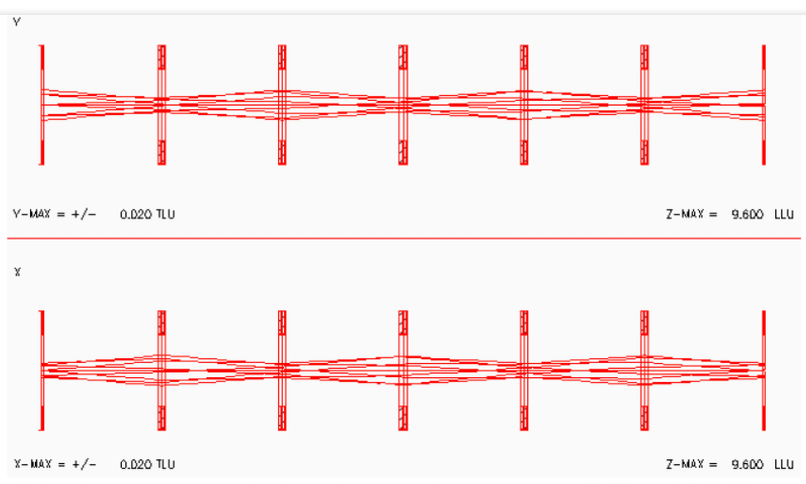

Fig. 91: Part of the beam optics design for medium-energy RIB (6 MeV/u, A=200, Z=79, Electrostatic Regidity = 30 MV, 5 π mm mrad) from CRYRING. The same periodic structure o electrostatic quadrupoles for low-energy RIB is used, but only one out of 4 elements is activated with a typical voltage of +-17 kV while three elements in between are turned off.

GSI TDR 2005

competition in FAIR LOIs

Comparison of proposals

	Exo+pbar (pbar-RI) TRAP	***pbar-A RING***
Measurable Quantity	n/p at surface	n/p at rms radius matter rms radii **
Drip-line Nuclides	O pion detection	X cold residue - unbound
Short-lived Nuclides	O 10 ms (Intensity >10^3 /s)	X beam cooling
Recoil Momentum	Δ requires accurate position measurements	O inverse kinematics
Feasibility	need evaluation, developments	established method

*** matter rms radii can be measured with (normal) protons*

M. Wada et al **P. Kinle et al**

Yell to

PUMA

Best & Unique Location:

CERN AD + CERN ISOLDE

Strong Collaboration:

Lead by Alexandre

Possible X-ray measurements:

Xenon TPC ?